



PCCP

Factors Controlling the Molecular Modification of One-Dimensional Zeolites

Journal:	<i>Physical Chemistry Chemical Physics</i>
Manuscript ID	CP-ART-06-2021-002619.R1
Article Type:	Paper
Date Submitted by the Author:	29-Jul-2021
Complete List of Authors:	Li, Rui; University of Houston, Department of Chemical and Biomolecular Engineering Elliott, William; Pennsylvania State University, Chemical Engineering Clark, R.; University of Houston, Department of Chemical and Biomolecular Engineering Sutjipto, James; University of Houston, Chemical and Biomolecular Engineering Rioux, Robert; Pennsylvania State University, Chemical Engineering Palmer, Jeremy; University of Houston, Chemical and Biomolecular Engineering Rimer, Jeffrey; University of Houston, Chemical and Biomolecular Engineering

SCHOLARONE™
Manuscripts

ARTICLE

Factors Controlling the Molecular Modification of One-Dimensional Zeolites

Received 00th January 20xx,
Accepted 00th January 20xx

Rui Li,^{a,b} William A. Elliott,^c R. John Clark,^b James G. Sutjianto,^b Robert M. Rioux,^{c,d*} Jeremy C. Palmer,^{b*} and Jeffrey D. Rimer^{b*}

DOI: 10.1039/x0xx00000x

Interactions between organic molecules and inorganic materials are ubiquitous in many applications and often play significant roles in directing pathways of crystallization. It is frequently debated whether kinetics or thermodynamics plays a more prominent role in the ability of molecular modifiers to impact crystal nucleation and growth processes. In the case of nanoporous zeolites, approaches in rational design often capitalize on the ability of organics, used as either modifiers or structure-directing agents, to markedly impact the physicochemical properties of zeolites. It has been demonstrated for multiple topologies that modifier-zeolite interactions can alter crystal size and morphology, yet few studies have distinguished the roles of thermodynamics and kinetics. We use a combination of calorimetry and molecular modeling to estimate the binding energies of organics on zeolite surfaces and correlate these results with synthetic trends in crystal morphology. Our findings reveal unexpectedly small energies of interaction for a range of modifiers with two zeolite structures, indicating the effect of organics on zeolite crystal surface free energy is minor and kinetic factors most likely govern growth modification.

Introduction

Organic-inorganic interactions are critical in many natural, biological, and synthetic crystallization processes.¹⁻⁴ Molecular modifiers are organic additives that possess an affinity for adsorbing on specific crystal (or amorphous precursor) interfaces and altering the anisotropic rate(s) of growth and/or assembly.^{5, 6} This technique has proven to be an effective and integral component of diverse processes in biomineralization^{7, 8}, ice inhibition⁹⁻¹², drugs for pathological diseases^{13, 14}, and materials engineering^{15, 16}. One of the most challenging aspects of selecting molecular modifiers for a particular material or application is the inability to predict its impact on crystal growth kinetics and the thermodynamic driving forces governing modifier adsorption on different crystal surfaces. A modifier's specificity to interact with particular crystal facets can be

governed by a range of modifier-crystal interactions (van der Waals, electrostatic, hydrogen bonding, and π - π stacking) and other factors (e.g. solvent ionic strength,¹⁷ and the ability of the modifier to displace solvent near the crystal surface^{18, 19}) that also contribute to modifier efficacy. Prior studies demonstrated modifiers can significantly alter zeolite crystal habit, thus providing a facile and highly versatile method to tailor crystal properties and optimize their performance in catalytic applications.^{20, 21} Studies examining the thermodynamics of small molecule adsorption on zeolites have predominantly focused on the gas phase²²⁻³³ with none, to our knowledge, characterizing the adsorption of molecular modifiers on zeolite surfaces.

Here we examine the effects of zeolite growth modifiers (ZGMs) using a combination of bulk crystallization assays, calorimetry measurements, and molecular modeling to characterize the thermodynamics of ZGM-zeolite interactions, and their influence on physical properties such as crystal size and morphology. We focus on two zeolites, ZSM-22 (**TON**) and zeolite L (**LTL**), which were selected on the basis of their commercial relevance as catalysts³⁴⁻⁴⁶ and their promise in photonics⁴⁷ and drug delivery⁴⁸ applications. The crystal structures of ZSM-22 (Fig. 1A) and zeolite L (Fig. 1B) both consist of one-dimensional straight channels with characteristic pore diameters of 5.1 and 7.5 Å, respectively. Crystals of ZSM-22 are more siliceous (Si/Al = 30 – 50)^{41, 49} than those of zeolite L (Si/Al = 2.6 – 3.3),²⁰ indicative of the Si-rich medium used to prepare ZSM-22 (Fig. S1, ESI[†]). The conditions used to synthesize ZSM-22⁴¹ and zeolite L^{20, 50} are based on reported protocols (see the Methods and Table S1, ESI[†]) that produce crystals with average Si/Al molar ratios of 34 and 3, respectively. Herein, we refer to

^a Beijing Key Laboratory for Green Catalysis and Separation, Department of Environmental Chemical Engineering, Beijing University of Technology, Beijing 100124, PR China.

^b Department of Chemical and Biomolecular Engineering, University of Houston, Houston, TX 77204, USA.

^c Department of Chemical Engineering, The Pennsylvania State University, University Park, PA 16801, USA

^d Department of Chemistry, The Pennsylvania State University, University Park, PA 16801, USA

*Corresponding Authors:

Jeffrey D. Rimer Email: jrimer@central.uh.edu

Jeremy C. Palmer Email: jcpalmer@uh.edu

Robert M. Rioux Email: rmr189@psu.edu

[†]Electronic Supplementary Information (ESI) available: Details of materials characterization, synthesis conditions, and simulation methods; powder XRD patterns; additional SEM images; description of the solution calorimeter; raw calorimetry and modelling data; and molecular information of ZGMs (PDF). See DOI: 10.1039/x0xx00000x

changes in crystal morphology on the basis of aspect ratio (AR), which is measured as the length of the longest dimension (*c*-direction for both zeolites) divided by that of the diameter.

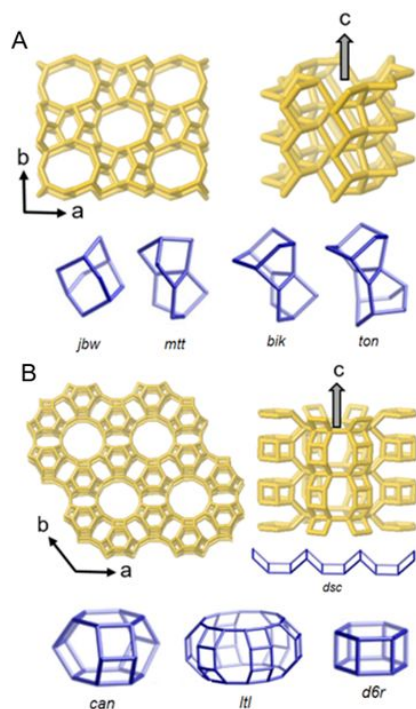


Fig. 1 Zeolite crystal structures. (A) ZSM-22 (TON framework) is a medium-pore zeolite (*Cmcm* space group) with 10-membered-ring channels (pore aperture = 4.6×5.7 Å) and unit cell parameters $a = 14.11$, $b = 17.84$, and $c = 5.26$ Å. (B) Zeolite L (LTL framework) is a large-pore zeolite (*P6/mmm* space group) with 12-membered-ring pore aperture (ca. 7 Å) and unit cell parameters $a = 18.13$, $b = 18.13$, and $c = 7.57$ Å. Each structure is comprised of distinct composite building units: TON (*jbw*, *mtt*, *bik*, *ton*) and LTL (*can*, *ltl*, *d6r*, *dsc*).

Methods

Here we briefly summarize the protocols used for zeolite crystallization, calorimetry measurements, and molecular modeling. More detailed experimental and computational methods are provided in the ESI†.

Zeolite Crystallization

ZSM-22 zeolites were synthesized with 1,8-diaminoctane (C_8DN) as an organic structure-directing agent (OSDA). Growth mixtures were prepared with a molar composition of $1 Al_2O_3 \cdot 90 SiO_2 \cdot 11.9 K_2O \cdot 27.3 C_8DN \cdot 3588 H_2O$. The mixture was aged at room temperature for ca. 21 h and was then placed in a Teflon-lined stainless steel acid digestion bomb and heated under rotation at 34 rpm in an oven at $160^\circ C$ and autogenous pressure. Zeolite L was synthesized in the absence of an organic using K^+ as an inorganic structure-directing agent (SDA). Growth mixtures were prepared with a molar ratio of $0.5 Al_2O_3 \cdot 20 SiO_2 \cdot 10.2 K_2O \cdot 1030 H_2O$. The mixture was aged at room temperature for ca. 21 h and was then placed in a Teflon-lined stainless steel acid digestion bomb and heated at $180^\circ C$ and autogenous pressure. For all zeolite syntheses with a ZGM, the

modifier was added 2 h prior to the finish of the aging period prior to hydrothermal treatment.

Calorimetry Studies

Calorimetry measurements were made on a semi-adiabatic solution calorimeter (TAMIII Precision Solution Calorimeter, TA Instruments) maintained at $25.0000 \pm 0.0001^\circ C$. The zeolite was dried under flow of helium at $400^\circ C$ for 4 h with a ramp rate of $2^\circ C/min$. Zeolite powder (20 mg) stored under nitrogen was placed in a 1 mL glass ampoule and sealed. The ampoule was submerged in a reaction vessel containing the wetting solution. Wetting solutions were prepared by combining a ZGM with a 0.1 M KOH aqueous solution. Each solution calorimetry utilizes ca. 20 mg zeolite, which led to the following amounts of ZGM (per gram zeolite): 0.81 mol ethanol, 0.60 mol ethylene glycol, 0.51 mol butanol, 0.41 mol glycerol, and 0.42 mol butanediols included in the basic solution. The ampoule was broken while continuously stirring. The change in temperature associated with the wetting event was measured and converted to enthalpy change using the average heat capacity. Data are the average of 3 measurements and error bars span two standard deviations.

Molecular Modelling

Molecular dynamics (MD) simulations were performed using GROMACS 4.6.7⁵¹ to study the adsorption of selected ZGMs, from an aqueous phase, onto the crystallographic surfaces of an all-silica TON structured zeolite. The all-silica representation of the TON framework provides a suitable model for the synthesized ZSM-22 material, which has a measured Si/Al ratio of 34 and hence low Al content. For materials with lower Si/Al ratios, inclusion of Al in the models may be important for accurately predicting ZGM-zeolite interactions. The ZGMs were modeled using the generalized AMBER force field⁵², the zeolite frameworks were described with the ClayFF potential^{53, 54}, and the SPC/E model was used for water⁵⁵. These force fields have been successfully used to model water-silica interfaces⁵⁴ and the adsorption of organic molecules in zeolites⁵⁶. We have also employed these force field choices in our previous studies, where they were found to yield good agreement with X-ray diffraction measurements in predicting the occlusion of organic structure-directing agents in zeolites^{57, 58}. Force field parameters for modeling van der Waals interactions between unlike species were determined using standard Lorentz-Berthelot combining rules. Real-space van der Waals and Coulombic interactions were truncated using a cutoff of 0.9 nm. Long-range contributions to the electrostatic interactions were treated using the particle mesh Ewald method, with parameters chosen to ensure a relative error of less than 10^{-5} in the calculated energy. The equations of motion were integrated using a leap-frog scheme with a 2 fs time step, and temperature was maintained using a Bussi-Parrinello velocity-rescaling thermostat⁵⁹ with a 2 ps relaxation time constant. Umbrella sampling MD simulations were performed to compute the free energy (potential of mean force) profiles characterizing the adsorption of ZGMs to the external surfaces of TON. Additional

details regarding general modeling protocols, free energy calculations, and data analysis methods are provided in the ESI[†].

Results and discussion

The ZGMs selected for this study (Table S2, ESI[†]) are inspired by molecules previously tested for zeolite L and other frameworks.^{20, 21} For brevity, we use a nomenclature for ZGMs where alcohols are referenced as LN_{i,j,k} with L = P for primary alcohols, D for diols, and T for triols; and N refers to the total number of carbons in the alkyl chain with subscripts *i,j,k* referring to the location of the alcohol groups along the alkyl backbone. Amines and amino acids are referred to by their names or common abbreviations. The quantity of ZGM was selected based on a previous report²⁰ using molar ratios x ZGM:1.0 SiO₂ (where $x = 0.04 - 1.5$). Electron micrographs and powder X-ray diffraction (XRD) patterns of selected samples are shown in Fig. S2 and S3, ESI[†], respectively. Higher ZGM quantities were employed for select amines (e.g. triethylenetetramine, Fig. S4, ESI[†]), which did not demonstrate significant efficacy. In rare cases, the use of high ZGM concentration promoted the formation of a different crystalline phase, which were not observed under the conditions examined in the current study. In the absence of modifiers, ZSM-22 (Fig. 2A) and zeolite L (Fig. 2C) crystals have elongated rod-like and cylindrical morphologies, respectively. Zeolite L crystals are relatively monodisperse in size with an average axial [001] dimension of 3 μm , whereas ZSM-22 crystals exhibit a broader range of sizes and a minor fraction of spheroidal particles (Fig. 2A, red arrow).

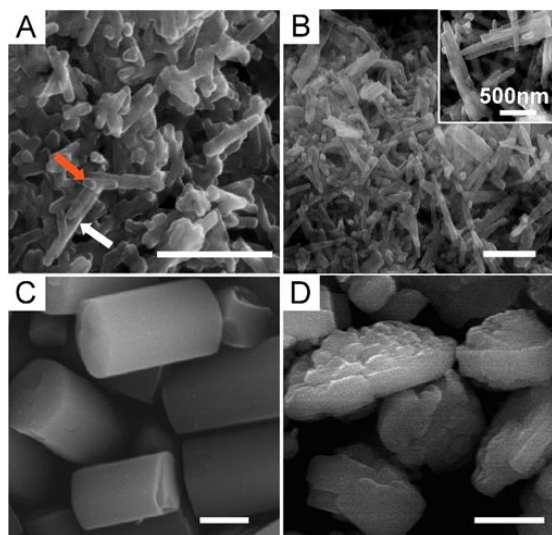


Fig. 2 Scanning electron micrographs of (A and B) ZSM-22 and (C and D) zeolite L crystals. Comparisons are made between the products of syntheses (A and C) in the absence of modifier (referred to as the control) and (B and D) in the presence of 1,3-butanediol (D_{4,1,3}, 1.5x the molar ratio of silica). Inset of B: high magnification image of representative ZSM-22 crystals. Arrows highlight the heterogeneous distribution of crystal size in as-synthesized ZSM-22 batches comprised of high AR rod-like crystals (A, white arrow) and small spheroidal crystals (A, red arrow). Scale bars equal 1 μm unless otherwise denoted.

In our previous study²⁰ we showed that ZGMs distinctly alter the anisotropic rates of zeolite L growth, leading to changes in crystal AR as a function of their hydrophobicity (Fig. 3A), which is quantified using the logarithm of the octanol-water partition coefficient ($\log P$) where values less than or greater than zero indicate hydrophilic or hydrophobic molecules, respectively. Introduction of ZGMs into synthesis mixtures of ZSM-22 results in smaller changes in crystal AR (Fig. 3B) compared to zeolite L. This is qualitatively consistent with previous studies reporting a greater sensitivity of zeolite L crystallization to synthesis parameters, such as water content or temperature,^{60, 61} compared to syntheses of ZSM-22. For example, subtle changes in synthesis parameters during the preparation of ZSM-22 can redirect growth to ZSM-11 (MEL), a common impurity (Table S3, ESI[†]).⁶² In the absence of ZGMs (*control*), the aspect ratio of crystals in this study (grey shaded regions in Fig. 3A and B) are consistent with the range of values reported in literature: ZSM-22 (AR = 5 – 20)^{63, 64} and zeolite L (AR \approx 2).²⁰ In the presence of ZGMs, there are clear trends in zeolite L morphology for select modifiers. For example, comparisons among homologous alcohols (e.g., primary alcohols or diols) reveals monotonic reductions in AR with increasing hydrophobicity (Fig. 3A); however, a broad comparison of different ZGMs with similar $\log P$ reveal that hydrophobicity is not a universal indicator of modifier efficacy. This was also confirmed for ZSM-22 synthesis where we observe no significant correlation between crystal AR and ZGM hydrophobicity (Fig. 3B). The large error bars reflect the polydisperse size distributions of ZSM-22 crystals. Within the confidence intervals of each experiment (i.e. error bars in Fig. 3B), there are no ZGMs that markedly reduce ZSM-22 crystal AR; however, there are several modifiers that lead to notable increases in AR.

In general, we observe the alcohols tested increase the ZSM-22 crystal AR, whereas amines have the opposite effect, in contrast to zeolite L where only minor differences are observed between alcohols and amines.²⁰ We also observe the effect of any one modifier on crystal morphology can be quite different for each zeolite structure. This is exemplified by syntheses in the presence of 1,3-butanediol (D_{4,1,3}) where the impact of the ZGM on crystal morphology is different for ZSM-22 (Fig. 2B) and zeolite L (Fig. 2D) in comparison to the controls (Fig. 2A and C, respectively). When evaluating the effect of various diols and triols, the positioning of alcohols along the carbon backbone is seemingly more impactful than the length of the carbon chain. This is evident when comparing crystal AR for diols of increasing length and fixed alcohol positions where there are appreciable differences in zeolite L crystal AR (D_{2,1,2} > D_{3,1,2} > D_{4,1,2} > D_{6,1,2}), but only minor variations in ZSM-22 crystal AR. The most significant changes in crystal morphology for both zeolites occur for diols with fixed chain length and varying alcohol position (listing trends in AR): zeolite L (D_{4,1,2} > D_{4,1,3} \approx D_{4,1,4}) and ZSM-22 (D_{4,1,3} \approx D_{4,1,4} > D_{4,1,2}). These observations indicate diols with hydroxyls located at either the (1,3) or (1,4) positions have a more pronounced impact on crystal morphology (relative to the control) than those with alcohols located at the (1,2) position. Similar observations for other minerals have been

reported, such the preferential adsorption of 1,3-diols on aluminates.^{20, 65} The adsorption of diols on zeolite crystal surfaces were examined in more detail by molecular modeling (*vide infra*).

To quantify the strength of ZGM adsorption on zeolite crystals, we performed solution (or immersion) calorimetry experiments for zeolite L (Table S4, ESI[†]) and ZSM-22 (Table S5, ESI[†]) to quantify the heat generated (or absorbed) by contacting calcined zeolite powders to an alkaline solution containing a fixed quantity of each modifier (Fig. S5, ESI[†]). The pH of the solution was adjusted using KOH to mimic the K⁺ ions

used as inorganic structure-directing agents in syntheses of both zeolite L and ZSM-22. During calorimetry measurements, the heat generated includes several phenomena such as solvation, dissociation of silanol groups in the presence of hydroxide ions, and the adsorption of K⁺ ions (or ion exchange) at negatively-charged sites located on bridging oxygens of Al-O-Si bonds or Al vacancies (i.e. SiO⁻K⁺ groups) within the zeolite framework. In

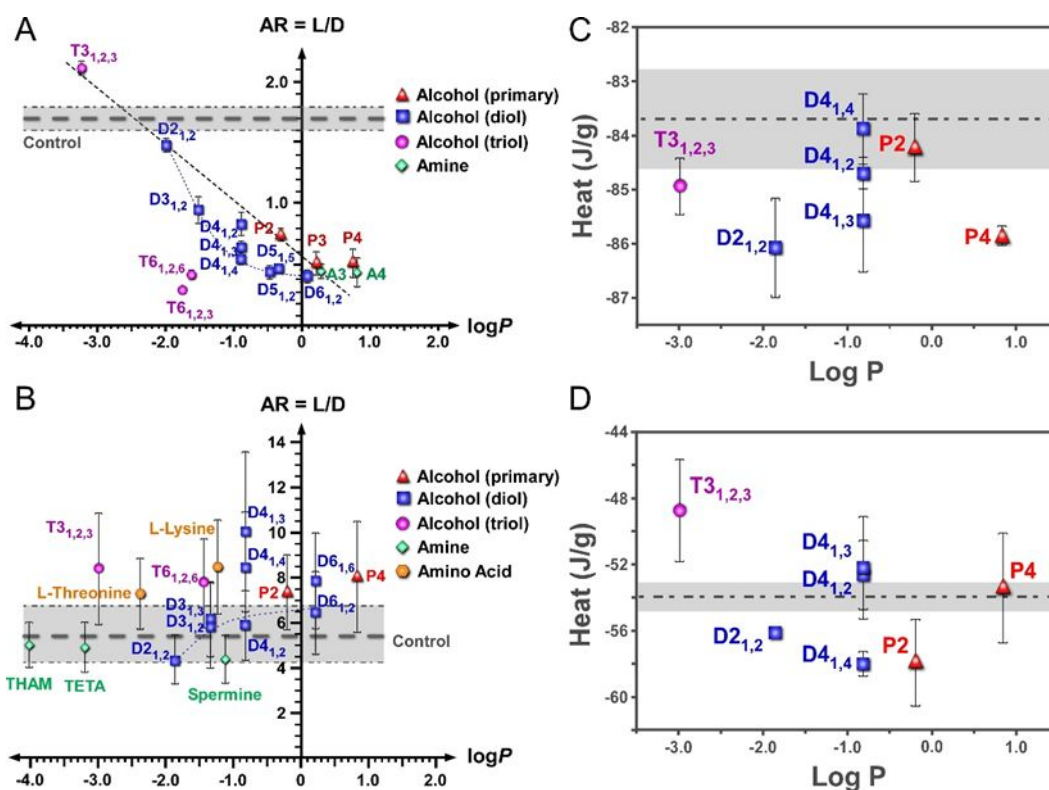


Fig. 3 (A and B) Aspect ratio, AR, of zeolite crystals as a function of modifier hydrophobicity (logarithm of the octanol-water partition coefficient, log P) for (A) zeolite L reported by Lupulescu et al.²⁰ (reprinted with permission by the American Chemical Society) and (B) ZSM-22 crystals. Each data point is the average of at least 80 measurements from electron micrographs, and error bars span two standard deviations. A molar ratio of x ZGM: SiO₂ was used in syntheses, where x = 0.04 for spermine, 0.06 for TETA and L-lysine, 0.07 for THAM and L-threonine, and 1.5 for all alcohols. (C and D) Calorimetry data for (C) zeolite L (Si/Al = 3) and (D) ZSM-22 (Si/Al = 35) in wetting solutions as a function of log P for selected modifiers. Wetting solutions were prepared by combining a ZGM with a 0.1 M KOH aqueous solution. Each solution calorimetry utilizes ca. 20 mg zeolite, which led to the following amounts of ZGM (per gram zeolite): 0.81 mol ethanol, 0.60 mol ethylene glycol, 0.51 mol butanol, 0.41 mol glycerol, and 0.42 mol butanediols included in the basic solution. Data are the average of 3 measurements and error bars span two standard deviations. Shaded grey regions in (A) – (D) correspond to experiments without ZGM; dashed lines indicate the average value and the width of the shaded region spans two standard deviations.

the presence of ZGMs, there is an additional heat of adsorption related to modifier interactions with the exterior or interior surfaces of zeolite crystals. Heat generation plotted as a function of modifier hydrophobicity for zeolite L (Fig. 3C) and ZSM-22 (Fig. 3D) reveal exothermic values spanning –46 to –87 J/g. It should be noted the absolute number or the identity of the species adsorbed to LTL or TON are unknown from heat of wetting experiments; the values presented in Figure 3C and D represent the overall energy change due to the adsorption of solvent, ZGMs and ions in solution. Heats of immersion are

larger for zeolite L, which may be attributed to differences in composition (i.e., zeolite L crystals have significantly higher Al content). Comparison of zeolite crystal AR and the heats of immersion show no apparent trends among alcohols selected for calorimetric analysis. We anticipated large changes in crystal morphology would be associated with higher heats of ZGM adsorption on crystal surfaces; however, this lack of complementarity suggests kinetic factors dominate the observed changes in crystal habit. More specifically, the observed changes in crystal shape are most likely dominated by

weak interactions between modifiers and the surfaces of zeolite crystals and/or growth units (i.e. monomer, (alumino)silicate oligomers, or amorphous precursors) to influence solute incorporation into growing crystals, thus altering the rate(s) of anisotropic crystal growth.

We have also examined potential relationships between crystal AR with the heats of immersion from calorimetry measurements of zeolite L (Fig. 4A) and ZSM-22 (Fig. 4B). An identical measurement was performed for each zeolite in the absence of modifier (using only 0.1 M KOH solution), which is depicted by the shaded grey regions. Interestingly, there is little difference in the magnitude of heat generation in the absence or presence of modifiers, indicating the adsorption of ZGMs on

zeolite surfaces is weak (i.e. 1 – 4 J/g) at room temperature. For measurements of ZSM-22, values for heat of immersion are less exothermic in the presence of some modifiers ($T3_{1,2,3}$) compared with the control KOH solution heat of immersion. This suggests an energetic penalty for displacing solvent from zeolite surfaces or hydrated protons, $H^+(H_2O)_n$, by modifiers. At the high temperatures employed in zeolite synthesis, it is likely modifier adsorption/desorption on zeolite crystals (or amorphous precursors) is rapid and reversible, leading to dynamic coverages of modifiers during crystallization. Heat of solution measurements contact a dry zeolite contained within an ampoule which is submerged in a ZGM-containing solution

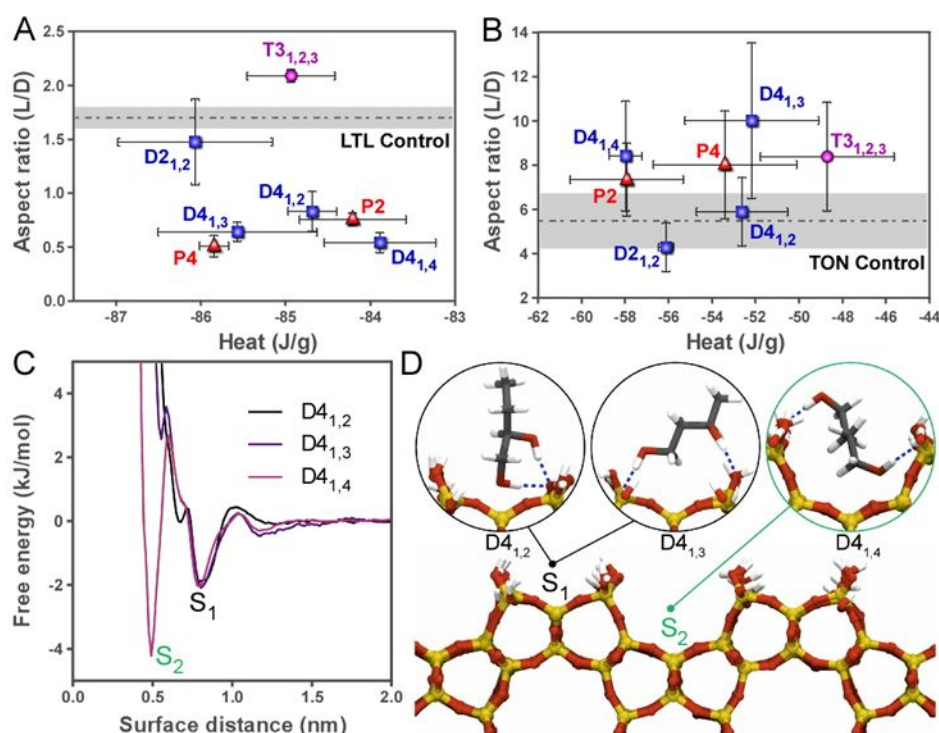


Fig. 4 (A and B) Heats of immersion (or wetting) as a function of crystal aspect ratio for (A) zeolite L and (B) ZSM-22 with select ZGMs. The shaded grey regions correspond to control samples (i.e., without ZGMs). (C) Free energy (potential of mean force) for butanediols ($D4_{1,2}$, $D4_{1,3}$, and $D4_{1,4}$) computed as a function of distance from the (010) surface of siliceous ZSM-22 using umbrella sampling molecular dynamics. Uncertainties in the free energy profiles are estimated to be less than 0.5 kJ/mol. (D) Favorable binding positions for the butanediols near features on the (010) surface formed from truncated 6- and 10-member rings (S_1 and S_2 , respectively). Movies S1 and S2, ESI[†] show $D4_{1,3}$ and $D4_{1,4}$ binding to S_1 and S_2 sites, respectively. Blue dashed lines show hydrogen bonds formed between the diols and surface silanols. Although the ZGMs adsorb from an aqueous phase in the simulations, the water molecules have been omitted from the visualizations for clarity.

by breaking ampoule (Fig. S5, ESI[†]). The calculated heat flow is typically normalized per gram since there is no simultaneous measure of the uptake or quantity sorbed, where sorption is inclusive of both adsorption and absorption. Heat of solution data in Fig. 3C and D clearly demonstrate the identity of the ZGM had little influence on the measured heat of wetting for the same zeolite, but the measured heat per gram value for a given ZGM differed between **TON** and **LTL** zeolites.

We attempted to convert the measured heat of wetting value to a more familiar enthalpy value based on the moles of ZGM adsorbed (see Supporting Text, ESI[†] for details). We could find no equilibrium adsorption isotherm characterization for alcohol adsorption from aqueous solution on the zeolites

selected for this study, but since **MOR** and **MFI** zeolites are structurally similar to **LTL** and **TON**, respectively, we additionally searched for references on **MOR** and **MFI**. Our literature search only found references for alcohol and diol sorption from aqueous solution into **MFI** (Table S6, ESI[†]). We were able to find adsorption from aqueous solution data for ethanol, 1-butanol, 1,2-butanediol, glycerol, and ethylene glycol,^{26, 27, 29, 66} but no data could be found for 1,3-butanediol or 1,4-butanediol. We utilized reported (or calculated) equilibrium adsorption constants for ZGMs to determine the amount sorbed based on the initial concentration of ZGM used in the current solution calorimetry experiments. Influenced by assumptions outlined in the ESI[†], calculated molar enthalpy values varied markedly

between the different ZGMs since literature-reported equilibrium adsorption constants varied significantly compared with to the measured heat of wetting values which were invariant with ZGM identity. Notably, 1,2-butanediol molar sorption enthalpies were calculated to be ca. -5 kJ/mol, consistent with the weak free energy calculated by molecular dynamics simulations (*vide infra*). Values for other ZGMs were larger in magnitude than 1,2-butanediol, but demonstrated a significantly greater span of calculated molar sorption enthalpies.

To characterize the molecular interactions of ZGMs with ZSM-22 crystal surfaces, we performed molecular dynamics (MD) simulations using butanediols ($D_{4,2}$, $D_{4,3}$, and $D_{4,4}$) that exhibited clear trends in their calorimetric heats of interaction. Given that modifiers tend to increase the aspect ratio of ZSM-22 crystals, which suggests preferential interactions of ZGMs with the sides of rod-like crystals, we selected the (010) surface as a representative termination. Using umbrella sampling MD (see the Methods, ESI† for details), we calculated the free energy (potential of mean force) as a function of the diol's center-of-mass-distance from the (010) surface of siliceous ZSM-22 (Fig. 4C). The small binding energies from MD simulations (ca. -2 to -4 kJ/mol) reveal ZGM interactions with the (010) surface are relatively weak. Whereas $D_{4,2}$ and $D_{4,3}$ have similar binding energies (ca. -2 kJ/mol), $D_{4,4}$ has slightly stronger interactions (ca. -4 kJ/mol), which is consistent with calorimetry measurements (Fig. 4B). Binding configurations (Fig. 4D) show the two alcohol groups on each diol form a hydrogen bond with exposed surface silanols (SiOH or SiO^-). The proximal spacing of these groups on $D_{4,2}$ and $D_{4,3}$ promotes binding atop of truncated 6-member ring (6-MR) features (labeled as S_1). The larger spacing of these groups on $D_{4,4}$, by contrast, leads to a more energetically favorable binding position in which the molecule forms hydrogen bonds with two adjacent 6-MRs and its center sits inside exposed channels formed from truncated 10-MRs (labelled as S_2). Similarly weak binding energies were found for each butanediol on the (100) and (001) surfaces of ZSM-22 (Table S7, ESI†), and in all cases entry into the pores was found to be thermodynamically unfavorable, confirming surface adsorption as the primary mode of interaction between the ZGMs and ZSM-22. This is qualitatively consistent with thermogravimetric analysis of select ZSM-22 samples prepared with various ZGMs showing negligible retention of organics in recovered solids (Fig. S6, ESI†).

The lack of distinct trends among ZGMs tested for ZSM-22 may be associated with the complex processes of zeolite crystallization.^{60, 67} While there are many possible mechanisms by which ZGMs can influence zeolite growth, their exact mode(s) of action are not well understood.⁶⁸ For many organic⁶⁹ or inorganic⁷⁰ crystals that grow predominantly by classical mechanisms (i.e., monomer addition), modifiers bind to surface sites (kinks, step edges, and/or terraces)^{3, 69, 71} and inhibit solute attachment by modes that include kink blocking^{72, 73} or step pinning^{74, 75}. Zeolites grow by a combination of classical and nonclassical mechanisms.⁷⁶ There is evidence suggesting ZGMs may act by a conventional mode of action involving the blocking

of growth sites on zeolite crystals,⁷⁷ although direct proof of this mechanism remains elusive. An alternative hypothesis is that ZGMs interact with diverse species in growth media that are involved in crystallization, such as soluble (alumino)silicates and amorphous precursors.^{78, 79} For instance, we recently showed organics (e.g. ZGMs and structure-directing agents) can switch the dominant mode of zeolite silicalite-1 (**MFI**) growth from particle attachment to monomer addition by suppressing the structural evolution of amorphous precursors.⁸⁰

In the present study, combined calorimetry measurements and MD simulations indicate weak interactions between ZGMs and zeolite crystal surfaces. This suggests ZGMs do not significantly alter the interfacial free energy of zeolite surfaces, which is the basis of thermodynamic arguments to postulate the effects of modifiers on crystal growth. The alternative argument seems more feasible: ZGMs impact the kinetics of crystallization via their ability to alter the physicochemical properties of growth units or regulate the rate of growth unit addition to zeolite crystals. It should be noted, however, quantifying the effects of ZGMs on the kinetics of crystallization with existing experimental techniques is nontrivial, if not impossible, owing to the complexity of dual classical and nonclassical pathways involved in zeolite formation.^{59, 68} Notably, zeolite growth solutions are comprised of diverse (alumino)silicate species ranging from monomers and oligomers to amorphous particles.^{76, 81-83} The identity of growth unit(s) and their relative contribution(s) to the rate of crystal growth are unknown, which makes the proposition of constructing a kinetic model currently unfeasible. Indeed, ZGMs have the capability of impacting zeolite growth through multiple processes that include (but are not limited to) the alteration of (alumino)silicate speciation, the assembly and/or structural evolution of amorphous precursors, and addition of these species (growth units) to crystal surfaces.^{60, 72} As such, there are many unanswered questions pertaining to the exact role of modifiers in zeolite synthesis that require fundamental insight on crystallization mechanisms before kinetic models can be established.

Conclusions

In summary, we have used a combination of experimental and modeling techniques to explore the impact of various organic modifiers on the crystallization of two commercially-relevant 1D zeolites. Our findings reveal apparent trends in ZGM efficacy, such as changes in crystal aspect ratio with modifier hydrophobicity, do not universally apply to all zeolites. To this end, there is no apparent correlation between the properties of modifiers and their impact on zeolite growth. Calorimetry measurements of both zeolite L and ZSM-22 samples reveal the enthalpy of modifier adsorption is small and sometimes endothermic. This is qualitatively consistent with the small modifier-zeolite binding energies calculated from MD simulations, which implies that adsorbed ZGMs are highly mobile on zeolite surfaces and can rapidly exchange between an adsorbed and desorbed state. Counter to thermodynamic-based hypotheses in literature, here we posit kinetics play a

more dominant role in zeolite crystal growth modification. Although the exact mechanisms of ZGMs in zeolite synthesis is not fully resolved, it is entirely possible that these organics exhibit more than one mode of action given the complexity of zeolite growth media as well as the broad variation in synthesis conditions among more than 245 known zeolite structures.

Author Contributions

Zeolite synthesis was performed by RL and JGS with JDR. Calorimetry measurements were performed by WAE with RMR. Molecular simulations were performed by RJC with JCP. The manuscript was written through the contributions of JDR, JCP, RMR, and RL. All authors have approved the final version of the manuscript.

Conflicts of interest

The authors declare no competing financial interests.

Acknowledgements

Primary support for this work comes from the National Science Foundation (DMREF Awards 1629398 and 1628960). JDR and JCP acknowledge additional support from The Welch Foundation (Awards E-1794 and E-1882, respectively). RL acknowledges additional support from the National Natural Science Foundation of China (Award 21908238). We also thank Ankur Agarwal for assistance with analyzing the simulation data.

Notes and references

- J. S. Seewald, *Nature*, 2003, **426**, 327.
- J. R. Young, J. M. Didymus, P. R. Brown, B. Prins and S. Mann, *Nature*, 1992, **356**, 516.
- J. Chung, I. Granja, M. G. Taylor, G. Mpourmpakis, J. R. Asplin and J. D. Rimer, *Nature*, 2016, **536**, 446.
- L. L. C. Olijve, K. Meister, A. L. DeVries, J. G. Duman, S. Guo, H. J. Bakker and I. K. Voets, *Proc. Natl. Acad. Sci. USA*, 2016, **113**, 3740.
- I. Weissbuch, M. Lahav and L. Leiserowitz, *Cryst. Growth Des.*, 2003, **3**, 125.
- I. Weissbuch, L. Addadi, M. Lahav and L. Leiserowitz, *Science*, 1991, **253**, 637.
- A. Dey, G. de With and N. A. J. M. Sommerdijk, *Chem. Soc. Rev.*, 2010, **39**, 397.
- J. W. Morse, R. S. Arvidson and A. Luttge, *Chem. Rev.*, 2007, **107**, 342.
- S. P. Graether, M. J. Kuiper, S. M. Gagne, V. K. Walker, Z. C. Jia, B. D. Sykes and P. L. Davies, *Nature*, 2000, **406**, 325.
- L. A. Graham and P. L. Davies, *Science*, 2005, **310**, 461.
- Y. C. Liou, A. Tocilj, P. L. Davies and Z. C. Jia, *Nature*, 2000, **406**, 322.
- F. D. Sonnichsen, B. D. Sykes, H. Chao and P. L. Davies, *Science*, 1993, **259**, 1154.
- J. D. Rimer, Z. An, Z. Zhu, M. H. Lee, J. A. Wesson, D. S. Goldfarb and M. D. Ward, *Science*, 2010, **330**, 337.
- L. N. Poloni and M. D. Ward, *Chem. Mater.*, 2014, **26**, 477.
- W. C. Huang, L. M. Lyu, Y. C. Yang and M. H. Huang, *J. Am. Chem. Soc.*, 2012, **134**, 1261.
- J. D. Rimer, M. Kumar, R. Li, A. I. Lupulescu and M. D. Oleksiak, *Catal. Sci. Technol.*, 2014, **4**, 3762.
- S. Farmanesh, B. G. Alamani and J. D. Rimer, *Chem. Commun.*, 2015, **51**, 13964.
- C.-L. Chen, J. Qi, R. N. Zuckermann and J. J. DeYoreo, *J. Am. Chem. Soc.*, 2011, **133**, 5214.
- S. Kerisit, S. C. Parker and J. H. Harding, *J. Phys. Chem. B*, 2003, **107**, 7676.
- A. I. Lupulescu, M. Kumar and J. D. Rimer, *J. Am. Chem. Soc.*, 2013, **135**, 6608.
- A. I. Lupulescu and J. D. Rimer, *Angew. Chem. Int. Ed.*, 2012, **51**, 3345.
- C. C. Lee, R. J. Gorte and W. E. Farneth, *J. Phys. Chem. B*, 1997, **101**, 3811.
- S. Savitz, F. Siperstein, R. J. Gorte and A. L. Myers, *J. Phys. Chem. B*, 1998, **102**, 6865.
- F. Eder and J. A. Lercher, *Zeolites*, 1997, **18**, 75.
- F. Eder and J. A. Lercher, *J. Phys. Chem. B*, 1997, **101**, 1273.
- E. E. Mallon, A. Bhan and M. Tsapatsis, *J. Phys. Chem. B*, 2010, **114**, 1939.
- E. E. Mallon, I. J. Babineau, J. I. Kranz, Y. Guefrachi, J. I. Siepmann, A. Bhan and M. Tsapatsis, *J. Phys. Chem. B*, 2011, **115**, 11431.
- R. Xiong, S. I. Sandler and D. G. Vlachos, *J. Phys. Chem. C*, 2011, **115**, 18659.
- R. Xiong, S. I. Sandler and D. G. Vlachos, *Langmuir*, 2012, **28**, 4491.
- P. Bai, M. Tsapatsis and J. I. Siepmann, *Langmuir*, 2012, **28**, 15566.
- X. Guo, P. Zhang and A. Navrotsky, *Micropor. Mesopor. Mater.*, 2020, **294**, 109893.
- W. E. Farneth and R. J. Gorte, *Chem. Rev.*, 1995, **95**, 615.
- R. J. Gorte and S. P. Crossley, *J. Catal.*, 2019, **375**, 524.
- G. Jacobs, W. E. Alvarez and D. E. Resasco, *Appl. Catal. A-Gen.*, 2001, **206**, 267.
- P. W. Tamm, D. H. Mohr and C. R. Wilson, in *Stud. Surf. Sci. Catal.*, ed. J. W. Ward, Elsevier, 1988, vol. Volume 38, pp. 335.
- R. D. Cortright and J. A. Dumesic, *Appl. Catal. A-Gen.*, 1995, **129**, 101.
- G. Li, T. Li and Y. Xu, *Chem. Commun.*, 1996, 497.
- J. Álvarez-Rodríguez, A. Guerrero-Ruiz, I. Rodríguez-Ramos and A. Arcoya-Martín, *Catal. Today*, 2005, **107–108**, 302.
- C. F. Parra, D. Ballivet and D. Barthomeuf, *J. Catal.*, 1975, **40**, 52.
- S. Teketel, U. Olsbye, K.-P. Lillerud, P. Beato and S. Svelle, *Micropor. Mesopor. Mater.*, 2010, **136**, 33.
- S. Teketel, W. Skistad, S. Benard, U. Olsbye, K. P. Lillerud, P. Beato and S. Svelle, *ACS Catal.*, 2012, **2**, 26.
- M. A. Asensi, A. Corma, A. Martínez, M. Derewinski, J. Krysciak and S. S. Tamhankar, *Appl. Catal. A-Gen.*, 1998, **174**, 163.
- R. Kumar and P. Ratnasamy, *J. Catal.*, 1989, **116**, 440.
- C. Martínez and A. Corma, *Coord. Chem. Rev.*, 2011, **255**, 1558.
- C. Perego and A. Carati, in *Zeolites: From Model Materials to Industrial Catalysts*, eds. J. Čejka, J. Pérez-Pariante and W. J. Roth, Transworld Research Network, 2008, pp. 357.
- United States Pat.*, US4556477, 1985.
- B. Schulte, M. Tsotsalas, M. Becker, A. Studer and L. De Cola, *Angew. Chem. Int. Ed.*, 2010, **49**, 6881.
- H. Lülfi, A. Bertucci, D. Septiadi, R. Corradini and L. De Cola, *Chem. Eur. J.*, 2014, **20**, 10900.
- F.-F. Wei, Z.-M. Cui, X.-J. Meng, C.-Y. Cao, F.-S. Xiao and W.-G. Song, *ACS Catal.*, 2014, **4**, 529.

- 50 A. Gaona-Gómez and C.-H. Cheng, *Micropor. Mesopor. Mater.*, 2012, **153**, 227.
- 51 B. Hess, C. Kutzner, D. van der Spoel and E. Lindahl, *J. Chem. Theory Comput.*, 2008, **4**, 435.
- 52 J. Wang, R. M. Wolf, J. W. Caldwell, P. A. Kollman and D. A. Case, *J. Comput. Chem.*, 2004, **25**, 1157.
- 53 R. T. Cygan, J.-J. Liang and A. G. Kalinichev, *J. Phys. Chem. B*, 2004, **108**, 1255.
- 54 O. Kroutil, Z. Chval, A. A. Skelton and M. Předota, *J. Phys. Chem. C*, 2015, **119**, 9274.
- 55 H. J. C. Berendsen, J. R. Grigera and T. P. Straatsma, *J. Phys. Chem.*, 1987, **91**, 6269.
- 56 N. Journal of Chemical Theory and Computation Jiang, M. Erdős, O. A. Moulton, R. Shang, T. J. H. Vlught, S. G. J. Heijman and L. C. Rietveld, *Chem. Eng. J.*, 2020, **389**, 123968.
- 57 A. Chawla, R. Li, R. Jain, R. J. Clark, J. G. Sutjianto, J. C. Palmer and J. D. Rimer, *Mol. Syst. Des. Eng.*, 2018, **3**, 159.
- 58 M. Kumar, Z. J. Berkson, R. J. Clark, Y. Shen, N. A. Prisco, Q. Zheng, Z. Zeng, H. Zheng, L. B. McCusker, J. C. Palmer, B. F. Chmelka and J. D. Rimer, *J. Am. Chem. Soc.*, 2019, **141**, 20155.
- 59 G. Bussi, D. Donadio and M. Parrinello, *J. Chem. Phys.*, 2007, **126**, 014101.
- 60 M. Kumar, R. Li and J. D. Rimer, *Chem. Mater.*, 2016, **28**, 1714.
- 61 A. K. Jamil, O. Muraza, M. Yoshioka, A. M. Al-Amer, Z. H. Yamani and T. Yokoi, *Ind. Eng. Chem. Res.*, 2014, **53**, 19498.
- 62 Y. Shen, T. T. Le, R. Li and J. D. Rimer, *ChemPhysChem*, 2018, **19**, 529.
- 63 F. Di Renzo, F. Remoué, P. Massiani, F. Fajula, F. Figueras and C. Thierry Des, *Zeolites*, 1991, **11**, 539.
- 64 Y. Wang, X. Wang, Q. Wu, X. Meng, Y. Jin, X. Zhou and F.-S. Xiao, *Catal. Today*, 2014, **226**, 103.
- 65 J. R. Copeland, X.-R. Shi, D. S. Sholl and C. Sievers, *Langmuir*, 2013, **29**, 581.
- 66 E. E. Mallon, M. Y. Jeon, M. Navarro, A. Bhan and M. Tsapatsis, *Langmuir*, 2013, **29**, 6546.
- 67 J. J. De Yoreo, P. U. P. A. Gilbert, N. A. J. M. Sommerdijk, R. L. Penn, S. Whitelam, D. Joester, H. Zhang, J. D. Rimer, A. Navrotsky, J. F. Banfield, A. F. Wallace, F. M. Michel, F. C. Meldrum, H. Cölfen and P. M. Dove, *Science*, 2015, **349**.
- 68 K. N. Olafson, R. Li, B. G. Alamani and J. D. Rimer, *Chem. Mater.*, 2016, **28**, 8453.
- 69 K. N. Olafson, M. A. Ketchum, J. D. Rimer and P. G. Vekilov, *Cryst. Growth Des.*, 2015, **15**, 5535.
- 70 S. Farmanesh, J. Chung, D. Chandra, R. D. Sosa, P. Karande and J. D. Rimer, *J. Cryst. Growth*, 2013, **373**, 13.
- 71 K. N. Olafson, M. A. Ketchum, J. D. Rimer and P. G. Vekilov, *Proc. Natl. Acad. Sci. USA*, 2015, **112**, 4946.
- 72 S. Elhadj, J. J. De Yoreo, J. R. Hoyer and P. M. Dove, *Proc. Natl. Acad. Sci. USA*, 2006, **103**, 19237.
- 73 J. J. De Yoreo and P. G. Vekilov, *Rev. Mineral. Geochem.*, 2003, **54**, 57.
- 74 T. Jung, X. Sheng, C. K. Choi, W.-S. Kim, J. A. Wesson and M. D. Ward, *Langmuir*, 2004, **20**, 8587.
- 75 J. F. Lutsko, N. González-Segredo, M. A. Durán-Olivencia, D. Maes, A. E. S. Van Driessche and M. Sleutel, *Cryst. Growth Des.*, 2014, **14**, 6129.
- 76 M. Kumar, M. K. Choudhary and J. D. Rimer, *Nat. Commun.*, 2018, **9**, 2129.
- 77 A. I. Lupulescu and J. D. Rimer, *Science*, 2014, **344**, 729.
- 78 R. Li, A. Smolyakova, G. Maayan and J. D. Rimer, *Chem. Mater.*, 2017, **29**, 9536.
- 79 A. I. Lupulescu, W. Qin and J. D. Rimer, *Langmuir*, 2016, **32**, 11888.
- 80 M. K. Choudhary, M. Kumar and J. D. Rimer, *Angew. Chem. Int. Ed.*, 2019, **58**, 15712.
- 81 R. Li, A. Chawla, N. Linares, J. G. Sutjianto, K. W. Chapman, J. G. Martínez and J. D. Rimer, *Ind. Eng. Chem. Res.*, 2018, **57**, 8460.
- 82 C. T. G. Knight, R. J. Balec and S. D. Kinrade, *Angew. Chem. Int. Ed.*, 2007, **46**, 8148.
- 83 J. M. Fedeyko, J. D. Rimer, R. F. Lobo and D. G. Vlachos, *J. Phys. Chem. B*, 2004, **108**, 12271.